photonics

MDPI

Communication

Investigation on Speckle-Free Imaging at the Output of a Multimode Fiber under Various Mode Excitation Conditions

Jun Zhou [1,2], Zichun Le [1,*], Yanyu Guo [1], Zongshen Liu [1], Qiyong Xu [1], Yanxin Dai [1], Jiayu Deng [1], Jiapo Li [1] and Di Cai [1]

[1] College of Science, Zhejiang University of Technology, Hangzhou 310023, China; zhoujun@cjlu.edu.cn (J.Z.); guoyanyu@szli.org (Y.G.); 2111909049@zjut.edu.cn (Z.L.); 2111909032@zjut.edu.cn (Q.X.); czdaiyx@sunnyoptical.com (Y.D.); dengjiayu@optiark.com (J.D.); 2111809049@zjut.edu.cn (J.L.); 2111909037@zjut.edu.cn (D.C.)

[2] College of Engineering Training Center, China Jiliang University, Hangzhou 310018, China

* Correspondence: lzc@zjut.edu.cn; Tel.: +86-130-8281-9650

Abstract: Speckle-free imaging using a multimode fiber has been widely used for imaging systems. Generally, previous work has assumed that all the propagating modes of the fiber are uniformly excited, but the modal power distribution is actually affected by excitation conditions. Here, we propose the utilization of a modal analysis method to study the dependence of the speckle contrast on the modal power distribution by changing the tilt angle of the Gaussian beam and on the group delay time difference caused by different fiber lengths. The results of numerical simulations and experiments show that, with an increase in the tilt angle of the Gaussian beam, the modal power is transferred to higher-order modes and the maximum delay difference between excitation modes becomes larger. Therefore, the inter-mode interference effect is effectively weakened, and the speckle contrast is significantly reduced. The increase in fiber length will also make the delay difference between excitation modes larger and thus the speckle contrast is decreased. For the larger tilt angle of the Gaussian beam, only a shorter optical fiber is required to reduce the speckle contrast significantly. Our work further promotes the use of a multimode fiber to produce speckle-free patterns in laser imaging systems.

Keywords: speckle-free image; multimode fiber; mode excitation

Citation: Zhou, J.; Le, Z.; Guo, Y.; Liu, Z.; Xu, Q.; Dai, Y.; Deng, J.; Li, J.; Cai, D. Investigation on Speckle-Free Imaging at the Output of a Multimode Fiber under Various Mode Excitation Conditions. *Photonics* **2021**, *8*, 171. https://doi.org/10.3390/photonics8050171

Received: 15 April 2021
Accepted: 19 May 2021
Published: 20 May 2021

1. Introduction

Laser light is widely used for imaging systems because it offers high brightness, a wide color gamut, high directionality, and a long lifetime [1–3]. However, when laser light with high coherence is transmitted through or reflected an optically rough object, speckle patterns produced by coherent waves interfering with each other are undesirable in many imaging applications, such as digital holographic microscopy [4], projection displays [5], optical coherence tomography [6], and synthetic aperture radar (SAR) imagery [7]. Speckles significantly deteriorate the image quality and have to be reduced to an extremely low value, or even speckle-free imaging is required.

Many approaches have been proposed to reduce speckle, such as a moving diffuser [8], screen movement [9], or a rotating light pipe [10], etc. Among them, the most popular method is to use moving diffraction optical elements (DOEs) [11,12], which enables efficient reduction in speckle, but the use of active moving elements will increase the power consumption and reduce the reliability of the systems.

Speckle reduction methods without active moving elements have also been developed. One of the attractive methods is to use a stationary multimode fiber. When a coherent laser is coupled into a multimode fiber, it will excite multiple modes with different propagation paths. Speckles can be reduced by destroying the laser temporal coherence by creating a sufficient delay difference among the fiber modes [13–15]. There are advantages of using

multimode fibers for speckle reduction, such as their low image transmission loss, flexibility and easiness for bending, and applicability to high-power lasers.

In previously published papers, speckle patterns at the output of a multimode fiber have been analyzed, and the related theories for speckle contrast calculation have been studied [16–19]. It has been found that the speckle contrast for a multimode fiber is essentially given by the impulse response of the fiber and the power spectrum of the source [20–22]. To reduce the speckle contrast of light emitting from a multimode fiber, one should enhance the intermodal dispersion by increasing the length or numerical aperture (*NA*) of the multimode fiber. However, the relationship between the speckle contrast at the output of a multimode fiber and the interference among excitation modes has not been clearly revealed in the studies mentioned above. Moreover, most of the work assumes that all propagating modes of the fiber are uniformly excited (equal intensity), but the modal power distribution is actually affected by excitation conditions. It is well known that all propagating modes of a fiber are non-uniform modal distributions when a tilted Gaussian-shaped coherent laser beam is launched into a multimode fiber. The modal power distribution has a crucial impact on the speckle formation. Therefore, it is necessary to study the relationship between the speckle contrast at the output of a multimode fiber and inter-mode interference under various excitation conditions.

In this paper, firstly, the modal power distributions under different excitation conditions in a weakly guided multimode fiber were theoretically investigated. Additionally, various modal power distributions could be realized by changing the tilt angle of the Gaussian beam. Subsequently, a modal analysis method was employed to derive general expressions for the speckle contrast at the output of a multimode fiber, which revealed that the speckle contrast is related to the power excitation coefficient and spatial configuration of guided modes, the group delay time difference (intermodal dispersion), and the temporal coherence of the laser source. Finally, numerical simulations and experiments were conducted to investigate the dependence of the speckle contrast on the modal power distribution by changing the tilt angle of the Gaussian beam and on the group delay time difference caused by different fiber lengths.

2. Theoretical Analysis

2.1. Various Modal Power Distribution by Varying the Tilt Angle of the Gaussian

For simplicity, we consider a step-index multimode fiber with a small index difference ($\Delta = (n_1 - n_2)/n_1 \ll 1$) under a weakly guided condition [23,24], where n_1 and n_2 are the refractive indexes of the core and cladding, respectively. For an incident Gaussian-shaped laser beam at the incident end of the multimode fiber ($z = 0$), the expression in the cylindrical coordinate system (r, ϕ, z) can be written as follows:

$$E_{in}(r,\phi) = \frac{1}{\rho} exp\left[-\frac{r^2}{\rho^2}\right] exp(-ik\theta rcos\phi) \quad (1)$$

where ρ is the Gaussian beam radius at the waist, $k = 2\pi/\lambda$ is the wave number in free space, λ is the wavelength, and θ is the angle of the incident Gaussian beam relative to the optical fiber axis. The paraxial approximation from Equation (1) is used so that the tilt angle θ of the Gaussian beam is only restricted to a very small range.

The incident Gaussian beam on the multimode fiber allows only the transmission of a light field coupled into the linearly polarized (LP) modes in the fiber. Therefore, the incident Gaussian beam is expressed as a superposition of modal fields as given below [25]:

$$E_{in}(r,\phi) = \sum_m \sum_n \alpha_{mn} LP_{mn}(r,\phi) \quad (2)$$

where m and n are the indices of the LP_{mn} mode and α_{mn} is the modal field amplitude excitation coefficient that is given by the following:

$$\alpha_{mn} = \int_0^{2\pi} \int_0^{+\infty} LP_{mn}^*(r,\phi) E_{in}(r,\phi) r dr d\phi \tag{3}$$

where the asterisk denotes the complex conjugate. Equation (3) can be further normalized, and the power excitation coefficient of the LP_{mn} mode can be obtained as follows:

$$\eta_{mn} = \frac{\left| \int_0^{2\pi} \int_0^{+\infty} LP_{mn}^*(r,\phi) E_{in}(r,\phi) r dr d\phi \right|^2}{\int_0^{2\pi} \int_0^{+\infty} |LP_{mn}(r,\phi)|^2 r dr d\phi \times \int_0^{2\pi} \int_0^{+\infty} |E_{in}(r,\phi)|^2 r dr d\phi}, 0 \le \eta_{mn} \le 1 \tag{4}$$

The modal field of LP_{mn} at the incident end (z = 0) of the step-index multimode fiber can be expressed as follows [26]:

$$LP_{mn}(r,\phi) = \begin{cases} A \frac{1}{J_m(U)} J_m\left(\frac{Ur}{a}\right) cos(m\varphi) & r \le a \\ A \frac{1}{K_m(W)} K_m\left(\frac{Wr}{a}\right) cos(m\varphi) & r \ge a \end{cases} \tag{5}$$

where A is a constant, a is the core radius, and J_m and K_m are the Bessel and modified Hankel functions of order m, respectively. U is the normalized transverse propagation constant of the fiber core ($r \le a$), and W is the normalized transverse propagation constant of the fiber cladding ($r \ge a$), which can be expressed as follows:

$$\begin{aligned} U &= a\left(k^2 {n_1}^2 - \beta^2\right)^{\frac{1}{2}} \\ W &= a\left(\beta^2 - k^2 {n_2}^2\right)^{1/2} \\ V^2 &= U^2 + W^2 = a^2 k^2 \left(n_1^2 - n_2^2\right) \end{aligned} \tag{6}$$

where V is the normalized frequency and β is the propagation constant along the direction of the fiber axis. According to the boundary conditions of the modal field, it must satisfy the following eigenvalue equation [24]:

$$\begin{cases} \frac{J_0(U)}{UJ_1(U)} = \frac{K_0(W)}{WK_1(W)}, m = 0 \\ \frac{J_m(U)}{UJ_{m-1}(U)} = -\frac{K_m(W)}{WK_{m-1}(W)}, m \ge 1 \end{cases} \tag{7}$$

The eigenvalue equation (Equation (7)) is a transcendental equation that must be solved numerically. The solution of the eigenvalue equation provides a set of discrete β_{mn} values, each of which corresponds to a specific modal field of linear polarization (LP_{mn}). Therefore, by using Equations (1), (5) and (7) and substituting them in Equation (4), we can obtain the modal power distributions under various excitation conditions (primarily by varying the tilt angle θ of the Gaussian beam).

2.2. Calculation of the Speckle Contrast at the Output of a Multimode Fiber

When a coherent light source is incident on a multimode fiber, a speckle field is formed at the output of the multimode fiber because of the interference among many guided modes. Subsequently, the general expression of the speckle contrast in the multimode fiber is derived using the modal field analysis method.

The multimode fiber is assumed to be an ideal optical guide, with no geometrical imperfections, to achieve mode guiding without attenuation and mode coupling. The optical field that propagates through the fiber of length z under the weakly guiding

condition can be represented as a superposition of linearly polarized modes with their propagation constants $\beta_p(\omega)$ at an angular frequency ω. This can be written as follows:

$$E(r,\phi,z,t) = \sum_p \alpha_p E_p(r,\phi) \int_0^{+\infty} g(\omega) exp\{i[\omega t - \beta_p(\omega) z]\} d\omega \tag{8}$$

where p is a simplified representation of the specific LP_{mn} mode with modal index pairs (m, n); α_p and E_p (r, ϕ) are the modal amplitude excitation coefficient and the spatial configuration of mode p, respectively; and $g(\omega)$ is the spectrum of the source field at the frequency ω. Thus, the instantaneous intensity of the light field output can be written as follows:

$$\begin{aligned} |E(r,\phi,z,t)|^2 = & \sum_p \sum_q \alpha_p \alpha_q^* E_p(r,\phi) E_q^*(r,\phi) \int_0^{+\infty} \int_0^{+\infty} g(\omega) g^*(\omega') exp[i(\omega \\ & -\omega') t] \times exp[-i\{\beta_p(\omega) - \beta_q(\omega')\} z] d\omega d\omega' \end{aligned} \tag{9}$$

For the intensity of the light field output I (r, ϕ, z) integrated over the eye (or camera), resolution time longer than the period of optical beat angular frequencies (ω-ω'), its expression can be written as follows:

$$\begin{aligned} I(r,\phi,z) = & \int |E(r,\phi,z,t)|^2 dt \\ & = \sum_p \sum_q \alpha_p \alpha_q^* E_p(r,\phi) E_q^*(r,\phi) \int_0^{+\infty} G(\omega) exp[-i\{\beta_p(\omega) \\ & - \beta_q(\omega)\} z] d\omega \end{aligned} \tag{10}$$

where $G(\omega) = |g(\omega)|^2$ is the spectrum density of the light source that satisfies the following normalization condition:

$$\int_0^{+\infty} G(\omega) d\omega = 1 \tag{11}$$

The complex degree of the temporal coherence of the source field by the Fourier transform is given as follows:

$$\gamma(t) = \int_0^{+\infty} G(\omega) exp(-i\omega t) d\omega, \gamma(0) = 1 \tag{12}$$

The coherence time t_c of the source is defined by the following equation [27]:

$$t_c = \int_0^{+\infty} |\gamma(t)|^2 dt \tag{13}$$

The frequency-dependent propagation constant of the individual mode can be expanded in two terms of a Taylor series around the central frequency ω_0 as follows:

$$\begin{aligned} \beta_p(\omega) &= \beta_p(\omega_0) + \frac{1}{V_p}(\omega - \omega_0), \ \frac{1}{V_p} = \left.\frac{d\beta_p(\omega)}{d\omega}\right|_{\omega=\omega_0} \\ \beta_q(\omega) &= \beta_q(\omega_0) + \frac{1}{V_q}(\omega - \omega_0), \ \frac{1}{V_q} = \left.\frac{d\beta_q(\omega)}{d\omega}\right|_{\omega=\omega_0} \end{aligned} \tag{14}$$

where V_p and V_q are the group velocities of the p mode and q mode, respectively. By substituting Equation (14) in Equation (10) and using the relation of Equation (12), we can rewrite the light field intensity expression as follows:

$$I(r,\phi,z) = \sum_p \sum_q \alpha_p \alpha_q^* E_p(r,\phi) E_q^*(r,\phi) \left|\gamma(\tau_p - \tau_q)\right| exp\left[i\omega_0(\tau_p - \tau_q)\right] exp\left[-i\{\beta_p(\omega_0) - \beta_q(\omega_0)\}z\right] \quad (15)$$

where $\tau_p = z/V_p$ and $\tau_q = z/V_q$ are the group delay times of the p mode and q mode, respectively. With the assumption that the speckle intensity pattern evolution in time is a random process, the phases of the different modes are realized as statistically independent and uniformly distributed between 0 and 2π. The ensemble average of the relevant phase terms is given by the following:

$$\langle exp\left[-i\{\beta_p(\omega_0) - \beta_q(\omega_0)\}z\right]\rangle = \delta_{pq} \quad (16)$$

where $\delta_{pq} = 1$ and $\delta_{pq} = 0$ for $p = q$ and $p \neq q$, respectively. The average intensity is obtained from Equation (15) as given below:

$$\langle I(r,\phi,z)\rangle = \sum_p \left|\alpha_p\right|^2 \left|E_p(r,\phi)\right|^2 \quad (17)$$

Equation (17) can be interpreted as the direct sum of the intensities of each guided mode. Similarly, the second moment of the light field intensity is written as follows:

$$\langle I^2(r,\phi,z)\rangle = \sum_p \sum_q \sum_s \sum_j \alpha_p \alpha_q^* \alpha_s \alpha_j^* E_p(r,\phi) E_q^*(r,\phi) E_s(r,\phi) E_j^*(r,\phi) \left|\gamma(\tau_p - \tau_q)\right| \left|\gamma(\tau_s - \tau_j)\right| exp\left[i\omega_0(\tau_p - \tau_q)\right] exp\left[i\omega_0(\tau_s - \tau_j)\right] \times \langle exp\left[-i\{\beta_p(\omega_0) - \beta_q(\omega_0) + \beta_s(\omega_0) - \beta_j(\omega_0)\}z\right]\rangle \quad (18)$$

The ensemble average of the relevant phase terms in Equation (18) is given by:

$$\langle exp\left[-i\{\beta_p(\omega_0) - \beta_q(\omega_0) + \beta_s(\omega_0) - \beta_j(\omega_0)\}z\right]\rangle = \delta_{pq}\delta_{sj} + \delta_{pj}\delta_{qs} \quad (19)$$

Three cases with non-zero values can be obtained from Equation (19): (a) $p = q = s = j$, (b) $p = q$, $s = j$ ($p \neq j$), and (c) $p = j$, $q = s$ ($p \neq q$). Thus, the expression for the second moment of the light intensity in Equation (18) can be written as follows:

$$\langle I^2(r,\phi,z)\rangle = \sum_p \sum_q \left|\alpha_p\right|^2 \left|\alpha_q\right|^2 \left|E_p(r,\phi)\right|^2 \left|E_q(r,\phi)\right|^2 + \sum \sum_{p\neq q} \left|\alpha_p\right|^2 \left|\alpha_q\right|^2 \left|E_p(r,\phi)\right|^2 \left|E_q(r,\phi)\right|^2 \left|\gamma(\tau_p - \tau_q)\right|^2 \quad (20)$$

The quantitative measure of the speckle field at the output of a multimode fiber is characterized by the speckle contrast, which is defined as the ratio of the standard deviation of the intensity fluctuation to the mean intensity [28]. The speckle contrast (SC) can be represented as follows:

$$SC = \frac{\sigma_I}{\langle I(r,\ \phi,\ z)\rangle} = \frac{\sqrt{\langle I(r,\ \phi,\ z)^2\rangle - \langle I(r,\ \phi,\ z)\rangle^2}}{\langle I(r,\ \phi,\ z)\rangle} \quad (21)$$

The square of the average intensity in Equation (17) can be written as:

$$\langle I(r,\ \phi,\ z)\rangle^2 = \sum_p \sum_q \left|\alpha_p\right|^2 \left|\alpha_q\right|^2 \left|E_p(r,\phi)\right|^2 \left|E_q(r,\phi)\right|^2 \quad (22)$$

The numerator term of Equation (21) by using the Equations (20) and (22) can be expressed as follows:

$$\begin{aligned}\sigma_{\mathrm{I}} &= \sqrt{\langle I(r,\,\phi,\,z)^2\rangle - \langle I(r,\,\phi,\,z)\rangle^2} \\ &= \sum\sum_{p\neq q} |\alpha_p|^2 |\alpha_q|^2 |E_p(r,\phi)|^2 |E_q(r,\phi)|^2 |\gamma(\tau_p - \tau_q)|^2\end{aligned} \tag{23}$$

By substituting Equations (17) and (23) in Equation (21), the expression of the speckle contrast at the output of a multimode fiber can be obtained:

$$SC = \frac{\sqrt{\sum\ \sum_{p\neq q} |\alpha_p|^2 |\alpha_q|^2 |E_p(r,\phi)|^2 |E_q(r,\phi)|^2 |\gamma(\tau_p - \tau_q)|^2}}{\sum_p |\alpha_p|^2 |E_p(r,\phi)|^2} \tag{24}$$

Equation (24) shows that speckle contrast is related to the following quantities: the power excitation coefficient ($|\alpha_p|^2$ and $|\alpha_q|^2$), the modal spatial configuration (E_p (r, ϕ) and E_q (r, ϕ)), the group delay time difference between mode p and mode q ($\tau_p - \tau_q$), and the complex degree of temporal coherence of the source field $\gamma(t)$. The physical meaning of the complex degree of temporal coherence $\gamma(t)$ in Equation (24) can be described as the temporal coherence properties of an excited laser source. The coherence time t_c of the laser source has been given in Equation (13): $t_c = \int_0^{+\infty} |\gamma(t)|^2 dt$.

For a Gaussian-shaped laser source, the complex degree of temporal coherence can be written as follows:

$$\gamma(t) = exp\left(-\frac{\pi t^2}{2t_c^2}\right) exp(-i\omega_0 t) \tag{25}$$

Using Equation (25), the complex degree term of the temporal coherence in Equation (24) can be expressed as $|\gamma(\tau_p - \tau_q)|^2 = exp\left[-\frac{\pi(\tau_p - \tau_q)^2}{t_c^2}\right]$. If the group delay time difference $(\tau_p - \tau_q)$ is greater than the coherence time t_c, then $|\gamma(\tau_p - \tau_q)|^2 \approx 0$. Therefore, we can choose an appropriate fiber length L to ensure that the group delay difference between any two modes is greater than the coherence time, that the inter-mode interference does not exist, and that the speckle pattern does not appear.

3. Simulation Results and Discussion

3.1. Various Modal Power Distribution by Varying the Tilt Angle of the Gaussian Beam

To evaluate the modal power distribution under different excitation conditions, we altered the tilt angle θ of the Gaussian beam to obtain the normalized power excitation coefficient η_{mn} of each LP_{mn} mode using Equations (1)–(7).

In the simulation, we first use the MATLAB software (7.9.0 (R2009b), MathWorks, Natick, MA 01760-2098, USA) to numerically solve the eigenvalue equation of Equation (7), and the normalized transverse propagation constants U and W of each modal field of linear polarization (LP_{mn}) can be calculated. Then, the U and W values of each modal field are substituted into Equation (5); we can obtain the expression of each LP_{mn} modal field. Finally, the expressions of the LP_{mn} modal field and the incident field of the Gaussian beam (see Equation (1)) are simultaneously substituted into Equation (4) to solve the power excitation coefficient of the LP_{mn} mode.

The following parameters were used in the numerical simulation: $n_1 = 1.483$, $n_2 = 1.436$, a = 100 μm, $A = 1$, $\lambda = 0.53$ μm, waist radius of the Gaussian beam $\rho = 65$ μm, numerical aperture of the multimode fiber $NA = \sqrt{n_1^2 - n_2^2} = 0.37$, and normalized frequency $V = \frac{2\pi a}{\lambda} NA = 438.4$. Figure 1 shows the modal power distribution under different excitation conditions (by varying the tilt angle θ of the Gaussian beam).

The excitation modes are very sensitive to the tilt angle of the Gaussian beam. As shown in Figure 1a, when the Gaussian beam is at normal incidence, a substantial amount

of the excitation power of the multimode fiber is in LP_{01} mode ($\eta_{01} = 0.926$). As the tilt angle θ of the Gaussian beam is increased to 0.2° (as shown in Figure 1b), the excitation modes are concentrated in LP_{11}($\eta_{11} = 0.259$), LP_{02}($\eta_{02} = 0.211$), LP_{12}($\eta_{12} = 0.161$), LP_{21}($\eta_{21} = 0.148$), and LP_{01}($\eta_{01} = 0.087$). As the tilt angle of the Gaussian beam continues to be increased, the modal power is transferred to higher-order modes (as shown in Figure 1c,d).

However, the tilt angle of the Gaussian beam cannot be very large because the paraxial approximation is adopted in Equation (1). Meanwhile, as the tilt angle is increased, there will be a certain amount of energy loss when the Gaussian beam is coupled into the multimode fiber. Therefore, a maximum tilt angle of 1° is used in the simulation. The excitation modes and power excitation coefficients are listed in Table 1 (these fiber modes contain a large portion of the laser power).

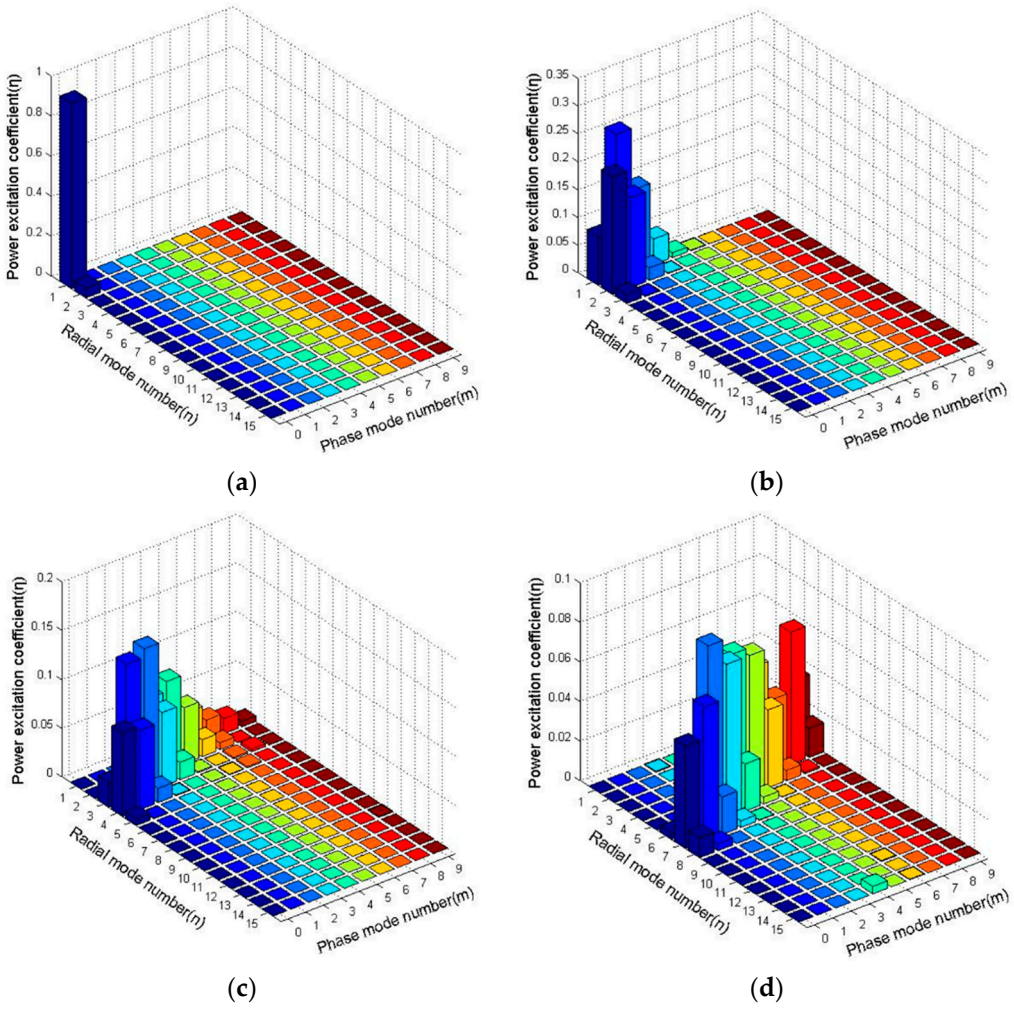

Figure 1. The modal power distributions under various excitation conditions (by varying the tilt angle θ of the Gaussian beam): (**a**) $\theta = 0°$; (**b**) $\theta = 0.2°$; (**c**) $\theta = 0.5°$; (**d**) $\theta = 1°$.

It can be seen from Table 1 that, with an increase in the tilt angle of the Gaussian beam, the excitation modes are transferred to higher-order modes and the modal power distribution will be changed. All the propagating modes of the fiber are not uniformly excited, and the modal power distribution is affected by excitation conditions. When the tilt angle of the Gaussian beam is coupled into a multimode fiber, several dominant modes of a multimode fiber are selectively excited and then propagate along the fiber.

Table 1. Excitation modes and power excitation coefficients by varying the tilt angle θ of the Gaussian beam.

Tilt Angle of the Gaussian Beam	Excitation Modes	Power Excitation Coefficient
$\theta = 0°$	LP_{01}	$\eta_{01} = 0.926$
$\theta = 0.2°$	LP_{11}	$\eta_{11} = 0.259$
	LP_{02}	$\eta_{02} = 0.211$
	LP_{12}	$\eta_{12} = 0.161$
	LP_{21}	$\eta_{21} = 0.148$
	LP_{01}	$\eta_{01} = 0.087$
$\theta = 0.5°$	LP_{23}	$\eta_{23} = 0.148$
	LP_{13}	$\eta_{13} = 0.139$
	LP_{42}	$\eta_{42} = 0.091$
	LP_{04}	$\eta_{04} = 0.085$
	LP_{32}	$\eta_{32} = 0.081$
	LP_{14}	$\eta_{14} = 0.081$
	LP_{33}	$\eta_{33} = 0.076$
$\theta = 1°$	LP_{26}	$\eta_{26} = 0.090$
	LP_{36}	$\eta_{36} = 0.078$
	LP_{45}	$\eta_{45} = 0.074$
	LP_{55}	$\eta_{55} = 0.070$
	LP_{17}	$\eta_{17} = 0.068$
	LP_{84}	$\eta_{84} = 0.067$
	LP_{64}	$\eta_{64} = 0.056$
	LP_{07}	$\eta_{07} = 0.052$

3.2. Speckle-Free Imaging under the Various Modal Power Distributions

It was shown in reference [22] that the presence of the speckle field at the output of the multimode fiber is related to the fiber length L. By changing the tilt angle of the Gaussian beam, various modal power distributions were obtained, as shown in Section 3.1. In this section, we calculate the required fiber length L under various modal power distributions to ensure that the group delay difference between any two modes is greater than the coherence time so that there is no interference, and speckle-free imaging can be achieved by using a sufficiently long multimode fiber.

The group delay time of the guide mode with the index values (m, n) to travel the length L of the multimode fiber is approximately given by the following expression [24]:

$$\begin{aligned}\tau_{mn} = \frac{L}{V_{mn}} = L\frac{d\beta_{mn}(\omega)}{d\omega} &= \frac{L}{c}\left\{\frac{d(n_2k)}{dk} + n_2\Delta\frac{d(Vb)}{dV}\right\} \\ &= \frac{L}{c}\left\{\frac{d(n_2k)}{dk} + n_2\Delta\left[1 - \left(\frac{U}{V}\right)^2\left(1 - 2\frac{K_m^2(W)}{K_{m-1}(W) \times K_{m+1}(W)}\right)\right]\right\}\end{aligned} \quad (26)$$

where c is the light velocity in a vacuum, and b is a normalized propagation constant, which is proportional to β and is defined by the following:

$$b = \frac{\frac{\beta}{k} - n_2}{n_1 - n_2} \quad (27)$$

The first and second parts of Equation (26) represent the material and waveguide dispersions, respectively. In a multimode fiber, the waveguide dispersion is generally dominant when compared to the material dispersion, and hence, the material dispersion

can be ignored. Therefore, the group delay time of the guide mode with the index values (m, n) can be approximated as follows:

$$\tau_{mn} \approx \frac{Ln_2\Delta}{c} \times \left[1 - \left(\frac{U}{V}\right)^2 \left(1 - 2\frac{K_m^2(W)}{K_{m-1}(W) \times K_{m+1}(W)}\right)\right] \tag{28}$$

According to reference [22], the maximum group delay time difference between the lowest order mode and the highest order mode supported by the fiber can be expressed as: $T_{\max} = \frac{L(NA)^2}{2n_1 c}$. For a step-index multimode fiber, the refractive index of the core $n_1 = 1.483$, the numerical aperture of the multimode fiber $NA = 0.37$, the speed of light in vacuum $c = 3.0 \times 10^8$ (m/s), thus $T_{\max}(\text{s}) = 153.85 \times 10^{-12}\ L$. However, when the tilt angle of the Gaussian beam is coupled into a multimode fiber, only several fiber modes are selectively excited and then propagate along the fiber. The excitation dominant modes at different tilt angles of the Gaussian beam have been listed in Table 1.

The normalized propagation constant b varies with the group delay time of excitation modes per unit length of fiber by using Equations (27) and (28) for the tilt angle $\theta = 0.2°$ and $0.5°$ of the Gaussian beams, as shown in Figure 2. It is obvious that the normalized propagation constant b of the low-order modes is larger than that of the higher-order modes. In addition, with an increase in the tilt angle of the Gaussian beam, the maximum delay difference between excitation modes becomes larger, which contributes to the reduction in speckle contrast.

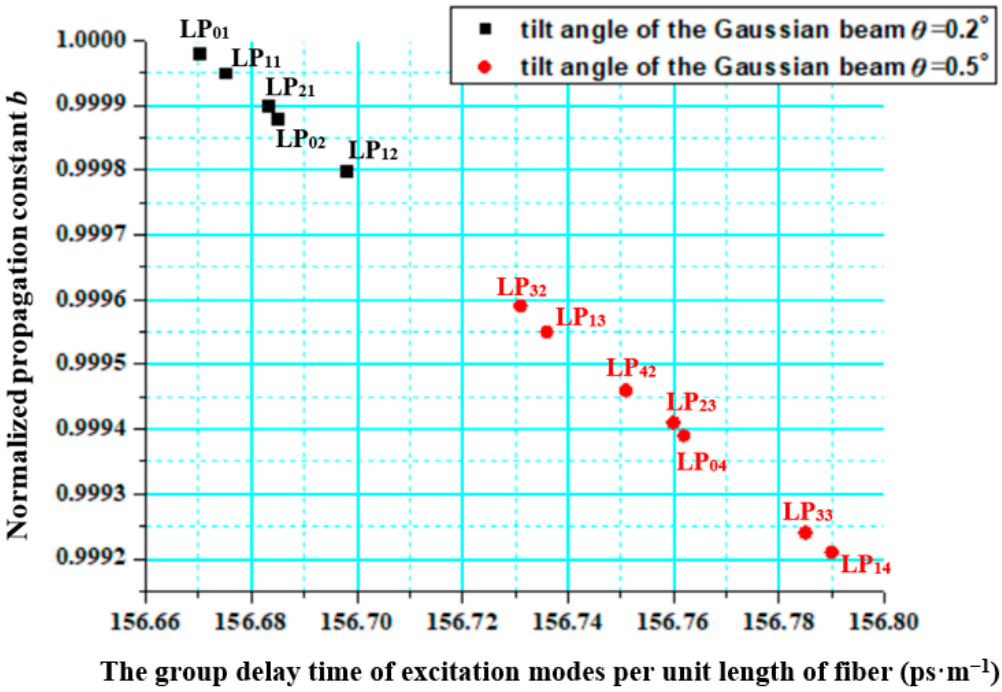

Figure 2. The normalized propagation constant b varies with the group delay time of excitation modes per unit length of fiber for the tilt angle $\theta = 0.2°$ and 0.5 of the Gaussian beams.

The group delay time of excitation modes for a tilt angle $\theta = 0.2°$ of the Gaussian beams in Table 1 can be calculated using Equation (28) as given below:

$$\begin{aligned}
&\text{LP}_{11}\text{: } U = 3.2129,\ W = 438.3882,\ \tau_{11}(\text{s}) = 156.675 \times 10^{-12}(\text{s}\cdot\text{m}^{-1}) \times L(\text{m});\\
&\text{LP}_{02}\text{: } U = 4.7652,\ W = 438.3741,\ \tau_{02}(\text{s}) = 156.685 \times 10^{-12}(\text{s}\cdot\text{m}^{-1}) \times L(\text{m});\\
&\text{LP}_{12}\text{: } U = 6.2146,\ W = 438.3559,\ \tau_{12}(\text{s}) = 156.698 \times 10^{-12}(\text{s}\cdot\text{m}^{-1}) \times L(\text{m});\\
&\text{LP}_{21}\text{: } U = 4.4569,\ W = 438.3773,\ \tau_{21}(\text{s}) = 156.683 \times 10^{-12}(\text{s}\cdot\text{m}^{-1}) \times L(\text{m});\\
&\text{LP}_{01}\text{: } U = 1.8893,\ W = 438.3959,\ \tau_{01}(\text{s}) = 156.670 \times 10^{-12}(\text{s}\cdot\text{m}^{-1}) \times L(\text{m}).
\end{aligned} \tag{29}$$

Then, the group delay time difference between any two modes can be calculated as follows:

$$\begin{array}{l} T_1 = |\tau_{11} - \tau_{02}| = 1.0 \times 10^{-14}(\mathrm{s{\cdot}m^{-1}}) \times L(\mathrm{m}); T_2 = |\tau_{11} - \tau_{12}| = 2.3 \times 10^{-14}(\mathrm{s{\cdot}m^{-1}}) \times L(\mathrm{m}); \\ T_3 = |\tau_{11} - \tau_{21}| = 0.8 \times 10^{-14}(\mathrm{s{\cdot}m^{-1}}) \times L(\mathrm{m}); T_4 = |\tau_{11} - \tau_{01}| = 0.5 \times 10^{-14}(\mathrm{s{\cdot}m^{-1}}) \times L(\mathrm{m}); \\ T_5 = |\tau_{02} - \tau_{12}| = 1.3 \times 10^{-14}(\mathrm{s{\cdot}m^{-1}}) \times L(\mathrm{m}); T_6 = |\tau_{02} - \tau_{21}| = 0.2 \times 10^{-14}(\mathrm{s{\cdot}m^{-1}}) \times L(\mathrm{m}); \\ T_7 = |\tau_{02} - \tau_{01}| = 1.5 \times 10^{-14}(\mathrm{s{\cdot}m^{-1}}) \times L(\mathrm{m}); T_8 = |\tau_{12} - \tau_{21}| = 1.5 \times 10^{-14}(\mathrm{s{\cdot}m^{-1}}) \times L(\mathrm{m}); \\ T_9 = |\tau_{12} - \tau_{01}| = 2.8 \times 10^{-14}(\mathrm{s{\cdot}m^{-1}}) \times L(\mathrm{m}); T_{10} = |\tau_{21} - \tau_{01}| = 1.3 \times 10^{-14}(\mathrm{s{\cdot}m^{-1}}) \times L(\mathrm{m}). \end{array} \quad (30)$$

Thus, the maximum delay difference and the minimum delay difference from Equation (30) are expressed as follows:

$$\begin{array}{l} T_{\max}(\mathrm{s}) = T_9 = 2.8 \times 10^{-14}(\mathrm{s{\cdot}m^{-1}}) \times L(\mathrm{m}), \\ T_{\min}(\mathrm{s}) = T_6 = 0.2 \times 10^{-14}(\mathrm{s{\cdot}m^{-1}}) \times L(\mathrm{m}). \end{array} \quad (31)$$

Consider that the coherence time t_c for a laser source with a spectral width Δv is $1/\Delta v$; a green semiconductor laser ($\lambda = 0.53$ μm) is used with a spectrum width of $\Delta\lambda = 2$ nm, and the coherence time $t_c = \lambda^2/(c\Delta\lambda) = 46.82 \times 10^{-14}$ (s). Comparisons of the coherence time t_c of the laser source with the maximum and minimum delay differences ($T_{\max}$ and $T_{\min}$) lead to the following three conditions:

1. $T_{\max} < t_c$: Interference occurs among all modes, and hence, the speckle contrast at the output of a multimode fiber is not significantly reduced. The optical fiber length L must be within 16.7 m.
2. $T_{\max} > t_c > T_{\min}$: Interference occurs among some modes, and hence, the speckle contrast at the output of a multimode fiber is significantly reduced. The optical fiber length L must be in the following range: 16.7 m < L < 234.1 m.
3. $T_{\min} > t_c$: Interference among all modes ceases, and hence, the speckle contrast at the output of a multimode fiber is equal to 0. The optical fiber length L must exceed 234.1 m.

To obtain speckle-free imaging, the length of the multimode fiber must exceed 234.1 m for the tilt angle $\theta = 0.2^\circ$ of the Gaussian beams. In a similar way, the group delay time of excitation modes and the required length of the multimode fiber are calculated as shown in Table 2 when the tilt angle is $\theta = 0.5^\circ$ and $\theta = 1^\circ$.

Table 2. The group delay time of excitation modes and the required length of the multimode fiber when the tilt angle of the Gaussian beam is $\theta = 0.5^\circ$ and $\theta = 1^\circ$, respectively.

Tilt Angle of the Gaussian Beam	Group Delay Time (s) of the Excitation Modes	Maximum Delay Difference $T_{\max}$ (s) and Minimum Delay Difference $T_{\min}$ (s)	The Degree of Speckle Reduction Corresponds to the Required Length of Multimode Fiber
$\theta = 0.5^\circ$	$\tau_{23} = 156.760 \times 10^{-12}L$ $\tau_{13} = 156.736 \times 10^{-12}L$ $\tau_{42} = 156.751 \times 10^{-12}L$ $\tau_{04} = 156.762 \times 10^{-12}L$ $\tau_{32} = 156.731 \times 10^{-12}L$ $\tau_{14} = 156.790 \times 10^{-12}L$ $\tau_{33} = 156.785 \times 10^{-12}L$	$T_{\max} = 5.9 \times 10^{-14}L$ $T_{\min} = 0.2 \times 10^{-14}L$	No significant reduction in speckle contrast: L < 7.9 m Significant reduction in speckle contrast: 7.9 m < L < 234.1 m Speckle-free imaging: L > 234.1 m
$\theta = 1^\circ$	$\tau_{26} = 156.993 \times 10^{-12}L$ $\tau_{36} = 157.042 \times 10^{-12}L$ $\tau_{45} = 156.984 \times 10^{-12}L$ $\tau_{55} = 157.030 \times 10^{-12}L$ $\tau_{17} = 157.048 \times 10^{-12}L$ $\tau_{84} = 157.057 \times 10^{-12}L$ $\tau_{64} = 156.969 \times 10^{-12}L$ $\tau_{07} = 156.995 \times 10^{-12}L$	$T_{\max} = 8.8 \times 10^{-14}L$ $T_{\min} = 0.2 \times 10^{-14}L$	No significant reduction in speckle contrast: L < 5.3 m Significant reduction in speckle contrast: 5.3 m < L < 234.1 m Speckle-free imaging: L > 234.1 m

It can be seen from Table 2 that, with an increase in the tilt angle of the Gaussian beam, the modal power is transferred to higher-order modes and the maximum delay difference between excitation modes becomes larger. Therefore, the inter-mode interference effect is effectively weakened, and the speckle contrast is significantly reduced. The increase in fiber length will also make the delay difference between excitation modes larger and thus the speckle contrast is decreased. For the larger tilt angle of the Gaussian beam, only a shorter optical fiber is required to reduce the speckle contrast significantly.

4. Experimental Results and Discussion

To verify the theoretical results shown above, an experimental setup based on the speckle contrast at the output of a multimode fiber under various excitation conditions (by varying the tilt angle of the Gaussian beam to θ = 0.2°, 0.5°, and 1°) was created, as illustrated in Figure 3. Multimode fibers of total length L = 2, 4, 7, 10, 15 and 20 m with a core diameter 2a = 200 μm and NA = 0.37 were used. A collimated green laser (λ = 0.53 μm) was incident on aperture D_1 = 1.3 mm, followed by a laser beam into the multimode fiber. One end of the fiber was mounted on a rotational stage so that the incident beam has a tilt angle θ relative to the optical fiber axis, and the other end was clamped by the optical fiber holder to ensure parallel output relative to the fiber axis. Subsequently, the output light of the multimode fiber was imaged on a screen through an objective lens with an aperture of D_2 = 50 mm and was finally captured by a Charge-coupled Device (CCD) camera.

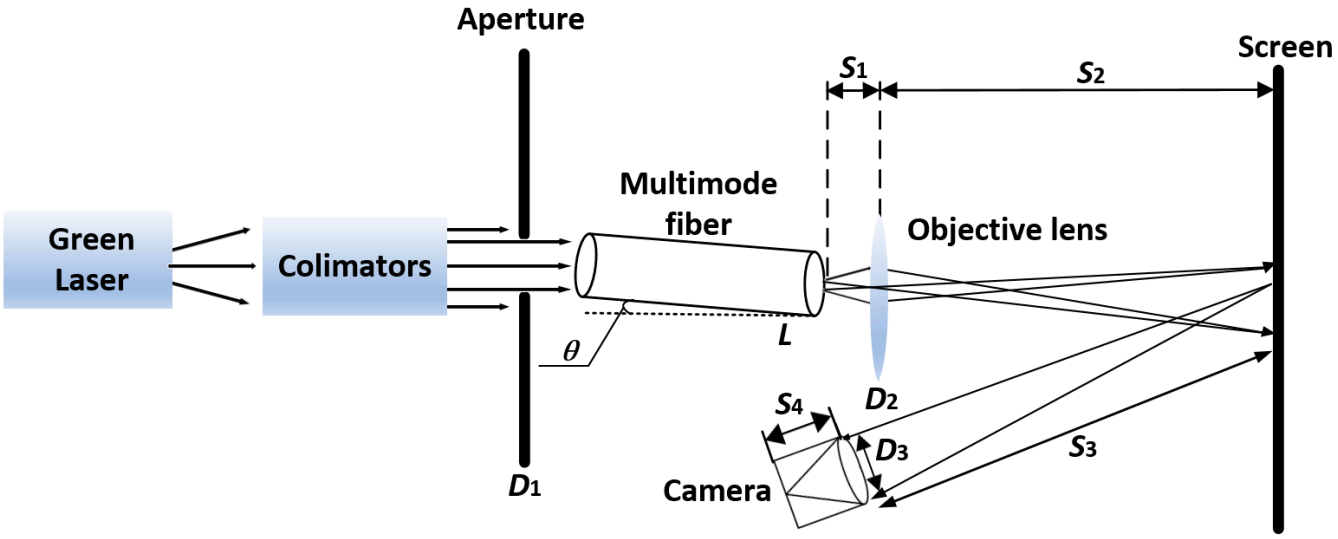

Figure 3. The experimental setup based on the speckle contrast at the output of a multimode fiber under various excitation conditions (by varying the tilt angle of the Gaussian beam to θ = 0.2°, 0.5°, and 1°). Here, D_1 = 1.3 mm, S_1 = 60 mm, D_2 = 50 mm, S_2 = 1800 mm, D_3 = 1 mm, S_3 = 1000 mm, and S_4 = 25 mm.

Figure 4 shows the speckle patterns and their one-dimensional (1D) intensity distributions when the incident angles of the Gaussian beam θ = 0.5° and 1° with a multimode fiber of length L = 7 m. As illustrated in Figure 4, as the tilt angle of the Gaussian beam was increased from θ = 0.5° to θ = 1°, the speckle contrast was reduced significantly and the speckle grain size became smaller. It can be clearly seen from the significant reduction in 1D intensity fluctuations that were extracted from the yellow line of the speckle patterns. This can be explained by the fact that, as the tilt angle of the Gaussian beam is increased, the modal power is transferred to higher-order modes and the maximum delay difference between excitation modes becomes larger. At this point, the inter-mode interference effect is effectively weakened. Therefore, the speckle contrast at the output of the multimode fiber is significantly reduced.

Figure 5 shows the relationship between the speckle contrast of the image captured by a CCD camera and the variation in the incident angle of the Gaussian beam under

multimode fibers with total length of L = 2, 4, 7, 10, 15, and 20 m. The comparison between experimental and theoretical results are given below.

According to the theoretical simulation and calculation, when the tilt angle of Gaussian beams is 0.2°, 0.5° and 1°, the required length for significant speckle reduction is L = 16.7 m, 7.9 m and 5.3 m, respectively. As illustrated in Figure 5, for the tilt angle of Gaussian beams is 0.2°, 0.5° and 1°, significant reduction in speckle contrast (steep curves segment) corresponding to the position range of fiber lengths are within 15 m–20 m, 7 m–10 m and 4 m–7 m. It can be concluded that for the larger tilt angle of the Gaussian beam, only a shorter optical fiber is required to reduce the speckle contrast significantly.

When fiber length L is less than the required length for significant speckle reduction (black curve segment with fiber length L < 15 m, red curve segment with fiber length L < 7 m, and blue curve segment with fiber length L < 4 m), the curves of speckle contrast decreased slowly. It can be theoretically explained that the group delay time difference between any excitation modes is less than the coherence time of the laser source, and the interference effect is not effectively weakened.

When fiber length L is great than the required length for significant speckle reduction (black curve segment with fiber length L > 15 m, red curve segment with fiber length L > 7 m, and blue curve segment with fiber length L > 4 m), the curves of speckle contrast decrease monotonically with fiber length L. Reference [22] shows the speckle contrast is inversely with $L^{1/2}$, which is consistent with our experimental results.

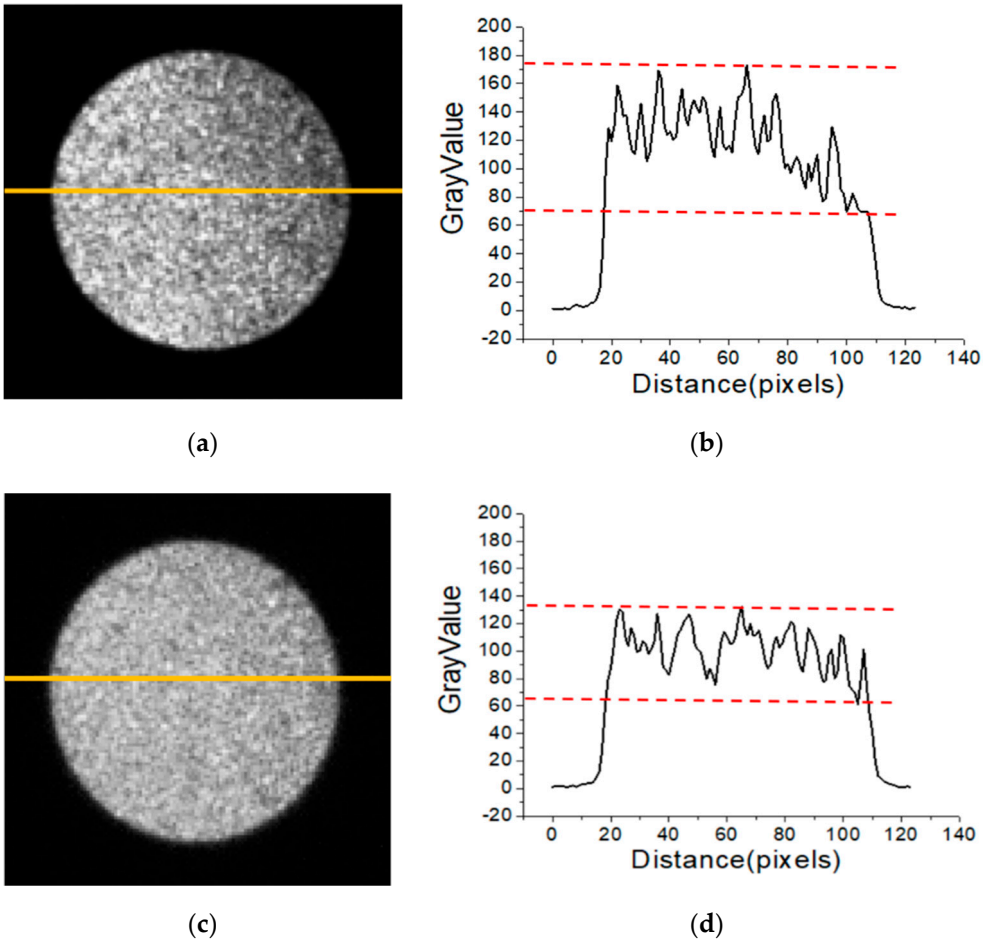

Figure 4. The speckle patterns and their 1D intensity distributions are shown when the incident angles of the Gaussian beam θ = 0.5° and 1° with a multimode fiber of length L = 7 m. (**a**) Speckle patterns under the condition of θ = 0.5° and L = 7 m, SC = 0.17; (**b**) 1D intensity distribution corresponding to (**a**); (**c**) speckle patterns under the condition of θ = 1° and L = 7 m, SC = 0.13; (**d**) 1D intensity distribution corresponding to (**c**). The 1D intensity distribution is extracted from the yellow line.

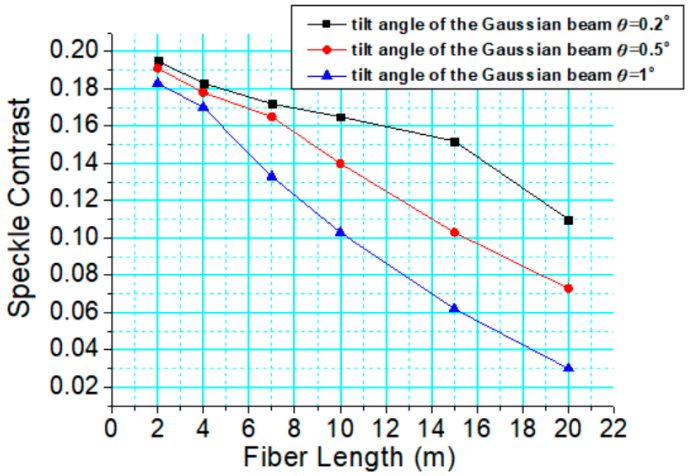

Figure 5. The speckle contrast from the image on the screen as a function of the incident angle θ = 0.2°, 0.5°, and 1° of the Gaussian beams with multimode fibers of total length L = 2, 4, 7, 10, 15, 20 m.

As can be seen from the asymptotic trend of the curves in Figure 5, the longer the fiber length is, the lower the speckle contrast can be, and eventually, speckle-free imaging can be obtained. However, in practical situations where a long multimode fiber is used, the fiber is generally coiled in a compact optical system. A small bending radius of optical fiber will lead to mode leakage and loss of light intensity, which will have an impact on speckle reduction. Reference [29] shows that if the distorted fundamental mode experiences sudden transition from straight fiber segment to bend fiber segment, the excitation of higher order modes could be ignored when the bend radius is larger than 200 mm. Meanwhile, when the bending radius/core radius (a = 100 μm) $\geq 10^3$, that is, the bending radius is greater than 100 mm, and the loss of light intensity due to bending is negligible. Therefore, the coiling radius of the multimode fiber is approximately 300 mm used in the experiment.

As focal ratio degeneration caused by the bending of the fiber, we can distinguish between higher order modes excited at the beginning of the fiber and during coiling/bending of the fiber by comparing whether the output focal ratio and the input focal ratio are equal. If the two are equal, it means that the higher order modes are excited at the beginning of the fiber. If the two are not equal, it means that the higher order modes are excited during coiling/bending of the fiber.

In order to avoid the influence of coiling/bending caused by using a long fiber, the compound speckle reduction scheme combining two or more speckle reduction approaches to achieve a better reduction effect has been proposed. According to Goodman's speckle theory [28], each speckle reduction effect from the compound speckle reduction method may be viewed as introducing a certain number of degrees of freedom. If we have r independent mechanisms for introducing new degrees of freedom, then the total number R of degrees of freedom is simply $R = \prod_{r=1}^{R} R_r$, and the total contrast of the resulting speckle is as follows: $SC = 1/\sqrt{R}$. For example, in our previous publications [14,15], the use of short multimode fibers with other static optical elements such as a two-dimensional Barker code diffractive optical element (DOE) could be a technical solution in speckle-free laser imaging systems.

In the fabrication process of the fiber, we should consider the existence of some defects, such as irregular boundaries of core-cladding interface, random fluctuation of refractive index, and random bending of optical fiber axis, which will also affect our experimental results.

Mode coupling takes place in an imperfect fiber waveguide. The variation in the power of the mth mode can be expressed as: $\Delta P_m = \sum_{n=1}^{M} h_{mn}(P_m - P_n)$, where P_{m} and P_{n} represent the initial power of the mth and nth modes, respectively. M is the total number of guided modes, and h_{mn} is the coupling coefficient between modes m and n. The higher order modes generated by mode coupling will play a positive role in averaging the speckle

patterns. In other words, the speckle contrast at the output end of the multimode fiber is decreased when the mode coupling occurs.

5. Conclusions

Speckle reduction using a multimode fiber has an important advantage in laser imaging systems because it is a passive method that does not increase power consumption or complicate the system. However, when a highly coherent laser is coupled with the multimode fiber, the modal power distribution is actually affected by the excitation conditions, which will have a crucial impact on speckle formation. Therefore, this article mainly investigated the relationship between the speckle contrast at the output of a multimode fiber and inter-mode interference under various excitation conditions. The modal field analysis method was employed to derive a general expression for the speckle contrast at the output of a multimode fiber under different excitation conditions by varying the tilt angle of the Gaussian beam. Moreover, numerical simulations were carried out to investigate the dependence of the speckle contrast on the modal power distribution by changing the tilt angle of the Gaussian beam and on the group delay time difference caused by different fiber lengths. The theoretical results obtained were confirmed by the experimental results. The results show that, with an increase in the tilt angle of the Gaussian beam, the modal power is transferred to higher-order modes and the maximum delay difference between excitation modes becomes larger. Therefore, the inter-mode interference effect is effectively weakened, and the speckle contrast is significantly reduced. The increase in fiber length will also make the delay difference between excitation modes larger and thus the speckle contrast is decreased. For the larger tilt angle of the Gaussian beam, only a shorter optical fiber is required to reduce the speckle contrast significantly. We anticipate that our work will facilitate the use of multimode fibers to produce speckle-free patterns in laser imaging systems.

Author Contributions: Conceptualization, J.Z. and Z.L. (Zichun Le); methodology, J.Z. and Z.L. (Zichun Le); software, J.Z. and Z.L. (Zongshen Liu); validation, Y.G., Q.X. and Y.D.; investigation, J.L. and D.C.; data curation, J.D.; writing—original draft preparation, J.Z.; writing—review and editing, Z.L. (Zichun Le); supervision, Z.L. (Zichun Le); funding acquisition, Z.L. (Zichun Le). All authors have read and agreed to the published version of the manuscript.

Funding: This research was funded by the National Natural Science Foundation of China (grant number 61975183), and the National Key R&D Program of China (grant numbers 2018YFB0504600 and 2018YFB0504603).

Institutional Review Board Statement: Not applicable.

Informed Consent Statement: Not applicable.

Data Availability Statement: Data is available from the corresponding author upon request.

Acknowledgments: J.Z. and Z.L. (Zichun Le) would like to thank A. Lapchuk for the valuable discussions.

Conflicts of Interest: The authors declare no conflict of interest.

References

1. Murayama, M.; Nakayama, Y.; Yamazaki, K.; Hoshina, Y.; Watanabe, H.; Fuutagawa, N.; Kawanishi, H.; Yemura, T.; Narui, H. Watt-class green (530 nm) and blue (465 nm) laser diodes. *Phys. Status Solidi A* **2018**, *215*, 1700513. [CrossRef]
2. Chellappan, K.V.; Erden, E.; Urey, H. Laser-based displays: A review. *Appl. Opt.* **2010**, *49*, F79–F98. [CrossRef]
3. Humeau-Heurtier, A.; Mahe, G.; Durand, S.; Abraham, P. Multiscale entropy study of medical laser speckle contrast images. *IEEE Trans. Biomed. Eng.* **2012**, *60*, 872–879. [CrossRef]
4. Feng, P.; Yang, L.; Wen, X. Coherent noise reduction in digital holographic microscopy by averaging multiple holograms recorded with a multimode laser. *Opt. Express* **2017**, *25*, 21815–21825.
5. Chen, H.; Pan, J.; Yang, Z. Speckle reduction using deformable mirrors with diffusers in a laser pico-projector. *Opt. Express* **2017**, *25*, 18140–18151. [CrossRef]

6. Ma, Y.; Chen, X.; Zhu, W.; Cheng, X.; Xiang, D.; Shi, F. Speckle noise reduction in optical coherence tomography images based on edge-sensitive cGAN. *Biomed. Opt. Express* **2018**, *9*, 5129–5146. [CrossRef]
7. Ai, J.; Liu, R.; Tang, B.; Jia, L.; Zhao, J.; Zhou, F. A refined bilateral filtering algorithm based on adaptively-trimmed-statistics for speckle reduction in SAR imagery. Biomed. *IEEE Access* **2019**, *7*, 103443–103455. [CrossRef]
8. Kubota, S.; Goodman, J.W. Very efficient speckle contrast reduction realized by moving diffuser device. *Appl. Opt.* **2010**, *49*, 4385–4391. [CrossRef] [PubMed]
9. Shin, S.C.; Yoo, S.S.; Lee, S.Y.; Park, C.; Park, S.; Kwon, J.W.; Lee, S. Removal of hot spot speckle on laser projection screen using both the running screen and the rotating diffuser. *J. Disp. Technol.* **2006**, *27*, 91–96. [CrossRef]
10. Sun, M.; Lu, Z. Speckle suppression with a rotating light pipe. *Opt. Eng.* **2010**, *49*, 024202. [CrossRef]
11. Lapchuk, A.; Kryuchyn, A.; Petrov, V.; Yurlov, V.; Klymenko, V. Full speckle suppression in laser projectors using two Barker code-type optical diffractive elements. *J. Opt. Soc. Am. A* **2013**, *30*, 22–31. [CrossRef] [PubMed]
12. Lapchuk, A.; Gorbov, I.; Le, Z.; Xiong, Q.; Lu, Z.; Prygun, O.; Pankratova, A. Experimental demonstration of a flexible DOE loop with wideband speckle suppression for laser pico-projectors. *Opt. Express* **2018**, *26*, 26188–26195. [CrossRef]
13. Ma, Q.; Xu, C.Q.; Kitai, A.; Stadler, D. Speckle reduction by optimized multimode fiber combined with dielectric elastomer actuator and light pipe homogenizer. *J. Disp. Technol.* **2016**, *12*, 1162–1167. [CrossRef]
14. Prygun, A.V.; Morozov, Y.M.; Kliuieva, T.Y.; Borodin, Y.A.; Le, Z. Completely passive method of speckle reduction utilizing static multimode fibre and two-dimensional diffractive optical element. *J. Mod. Opt.* **2019**, *66*, 1688–1694. [CrossRef]
15. Le, Z.; Lapchuk, A.; Guo, Y.; Dai, Y.; Gorbov, I. Investigation of speckle suppression beyond human eye sensitivity by using a passive multimode fiber and a multimode fiber bundle. *Opt. Express* **2020**, *28*, 6820–6834.
16. Imai, M.; Ohtsuka, Y. Speckle-pattern contrast of semiconductor laser propagating in a multimode optical fiber. *Opt. Commun.* **1980**, *33*, 4–8. [CrossRef]
17. Efimov, A. Spatial coherence at the output of multimode optical fibers. *Opt. Express* **2014**, *22*, 15577–15588. [CrossRef]
18. Efimov, A. Coherence and speckle contrast at the output of a stationary multimode optical fiber. *Opt. Lett.* **2018**, *43*, 4767–4770. [CrossRef]
19. Halpaap, D.; Tiana-Alsina, J.; Vilaseca, M.; Masoller, C. Experimental characterization of the speckle pattern at the output of a multimode optical fiber. *Opt. Express* **2019**, *27*, 27737–27744. [CrossRef]
20. Dandliker, R.; Bertholds, A.; Maystre, F. How modal noise in multimode fibers depends on source spectrum and fiber dispersion. *J. Lightwave Technol.* **1985**, *3*, 7–12. [CrossRef]
21. Hlubina, P. Spectral and dispersion analysis of laser sources and multimode fibers via the statistics of the intensity pattern. *J. Mod. Opt.* **1994**, *41*, 1001–1014. [CrossRef]
22. Manni, J.G.; Goodman, J.W. Versatile method for achieving 1% speckle contrast in large-venue laser projection displays using a stationary multimode optical fiber. *Opt. Express* **2012**, *20*, 11288–11315. [CrossRef] [PubMed]
23. Crosignani, B.; DiPorto, P. Coherence of an electromagnetic field propagating in a weakly guiding fiber. *J. Appl. Phys.* **1973**, *44*, 4616–4617. [CrossRef]
24. Gloge, D. Weakly guiding fibers. *Appl. Opt.* **1971**, *10*, 2252–2258. [CrossRef] [PubMed]
25. Snyder, A.W.; Young, W.R. Modes of optical waveguides. *J. Opt. Soc. Am.* **1978**, *68*, 297–309. [CrossRef]
26. Snyder, A.W.; Love, J.D. *Optical Waveguide Theory*; Chapman & Hall: New York, NY, USA, 1983.
27. Born, M.; Wolf, E. *Principles of Optics*, 7th ed.; Cambridge University Press: Cambridge, UK, 1999.
28. Goodman, J.W. *Speckle Phenomena in Optics: Theory and Applications*; Viva Books: New Delhi, India, 2008.
29. Li, J.; Wang, J.; Ding, Y.; Xu, D.; Lin, H.; Jing, F. Effect of fiber coiling mode on modes excitation. *Acta Opt. Sin.* **2011**, *31*, s100204.